Simple spinless mixed-valence model. I. Coherent-hybridization states versus virtual-bound states

P. Schlottmann
Institut für Theoretische Physik, Freie Universität Berlin, 1000 Berlin 33, Arnimallee 3, Germany
(Received 23 October 1979)

We consider a model consisting of spinless localized $4f$ levels interacting with spinless extended $5d$ states via a hybridization V and a local Coulomb repulsion U_{fd}. Using the renormalization-group technique we derive the scaling laws of the system within the leading and next-leading logarithmic approximation. We obtain that if $U_{fd} \ll V$ the mixed-valence states are extended and coherent, while if $U_{fd} \gg V$ the valence fluctuations are mainly local and incoherent.

I. INTRODUCTION

The electronic properties of mixed-valence systems are usually described by models assuming localized atomiclike f states and extended bandlike d states. These two types of states are mixed by a hybridization matrix element V and interact via interband and intraband Coulomb forces U. This class of models is known in the literature as the two-band Hubbard model or the Anderson lattice. The general Hamiltonian is the following:

$$H=\sum_{\vec{k}\sigma}\epsilon_k d^\dagger_{\vec{k}\sigma}d_{\vec{k}\sigma}+E\sum_{i\sigma}f^\dagger_{i\sigma}f_{i\sigma}+U_{ff}\sum_i f^\dagger_{i\uparrow}f_{i\uparrow}f^\dagger_{i\downarrow}f_{i\downarrow}$$
$$+V\sum_{i\sigma}(f^\dagger_{i\sigma}d_{i\sigma}+d^\dagger_{i\sigma}f_{i\sigma})+U_{fd}\sum_{i\sigma\sigma'}f^\dagger_{i\sigma}f_{i\sigma}d^\dagger_{i\sigma'}d_{i\sigma'}$$
$$-J\sum_{i\sigma\sigma'}f^\dagger_{i\sigma}S_{\sigma\sigma'}f_{i\sigma'}d^\dagger_{i\sigma'}s_{\sigma'\sigma}d_{i\sigma}, \qquad (1.1)$$

where $d^\dagger_{\vec{k}\sigma}$ is the creation operator for an extended d state with momentum $\vec{k}$ and spin σ,

$$d^\dagger_{i\sigma}=N^{-1/2}\sum_{\vec{k}}\exp(-i\vec{k}\cdot\vec{R}_i)d^\dagger_{\vec{k}\sigma},$$

$f^\dagger_{i\sigma}$ is the creation operation for a localized electron at site i with spin σ, N is the number of lattice sites, and $S_{\sigma\sigma'}$, $s_{\sigma\sigma'}$ are spin-$\frac{1}{2}$ matrices. The orbital degeneracy and the Coulomb repulsion between the d electrons have been neglected here.

This model has been extensively discussed within several approximation schemes as reviewed by Robinson.[1] The results, however, seem to depend quantitatively and even qualitatively on the employed approximation procedure.[1-10] In order to simplify the problem some special cases of this Hamiltonian have been considered:

(a) *The Falicov and Kimball model*[2,6] corresponds to Eq. (1.1) with $V=J=0$. Under these conditions the f electrons have no mobility and their spatial configuration is conserved. For sufficiently large U_{fd} couplings discontinuous charge transitions can be induced. The ground state is not spatially homogeneous; it shows magnetic as well as charge short-range and long-range order.[10] This case can be adapted to describe inhomogeneous mixed-valence compounds[11] (Sm_3S_4, Eu_3S_4) which are n-type semiconductors with a constant average number of f electrons per rare-earth ion, $n_f=\frac{1}{3}$.

(b) In the *narrow-band* limit[9] the atomic correlations are taken into account correctly, and perturbation is made with respect to the $5d$-electron hopping integral which is the small parameter.

The Hamiltonian, Eq. (1.1), shows two types of excitations, mixed and coupled, in a complicated way: charge transfer between the two bands and spin-flips, e.g., in the f level on one rare-earth ion. The model is considerably simplified by suppressing one type of excitation.

(c) The *Kondo lattice*[12,13] is obtained by assuming that the one-electron f states are far below the Fermi level ($\epsilon_F - E$ is large compared to V). Each rare-earth ion has one f electron and is characterized by its spin, whereas charge fluctuations are suppressed.

(d) The spin fluctuations cannot be eliminated by a special choice of parameters in Eq. (1.1), but by considering a model of *spinless fermions*.[14,15] Since most of the experiments probe the mixed-valence state via the magnetic moment, this artificial model is not supposed to explain the actual physical situation. This simple model, however, still has the main characteristics of a mixed-valence system, namely, the coexistence of two ionic states with similar energies, as well as some of its mathematical difficulties.

In this paper we discuss in more detail this latter case. From the interactions of the Hamiltonian, Eq. (1.1), only U_{fd} and V remain. Although neglecting the spins represents a large simplification, the problem still has the following technical complications:

(1) If U_{fd} is comparable to the bandwidth and V is small, the difficulties are similar to those of

the Hubbard model.

(2) For small U_{fd} and V the perturbation expansion with respect to U_{fd} for physical quantities (e.g., the vertex function, the self-energies) shows logarithmic infrared divergences similar to those in the Kondo problem and the interacting one-dimensional Fermi gas.

(3) The question of whether the valence fluctuations are extended and coherent, or local and incoherent.

In order to understand the latter question it is instructive to review briefly the Hartree-Fock solutions by Khomskii and Kocharjan[14] and by Leder[15]; the two approaches yielded quite different results. Both considered all possible factorizations including excitonlike correlations between f holes and d-band electrons:

$$U_{fd} f^\dagger f d^\dagger_{\vec{k}} d_{\vec{k}'} \to U_{fd}\left(\langle f^\dagger f\rangle d^\dagger_{\vec{k}} d_{\vec{k}'} + \langle d^\dagger_{\vec{k}} d_{\vec{k}'}\rangle f^\dagger f - \langle d^\dagger_{\vec{k}} f\rangle f^\dagger d_{\vec{k}'} - \langle f^\dagger d_{\vec{k}'}\rangle d^\dagger_{\vec{k}} f\right), \tag{1.2}$$

where the latter two terms were included into an effective hybridization. In one case[14] the enhancement of the hybridization was considered as local and incoherent among the rare-earth ions; i.e., they act like independent resonance levels. This picture yields discontinuous valence transitions for sufficiently large U_{fd}. On the other hand, in the case of extended valence fluctuations,[15] the coherence of the states opens a gap around the Fermi level and yields a large exciton condensation which smears possible discontinuities of n_f unless V is zero.

The rest of the paper is organized as follows. In Sec. II we give a brief survey of the renormalization-group technique,[16] and we define our model and the functions we need for the renormalization. In Sec. III we present the vertex renormalization in leading logarithmic order for both the extended and the local mixed-valence states. The detailed calculation up to next-leading logarithmic order follows in Secs. IV and V, respectively. A discussion of the results is given in Sec. VI.

In summary, we analyze the model for small U_{fd} and V within the leading and next-leading logarithmic approximation. We can conclude that:

(1) If $U_{fd} \ll V$ the valence fluctuations are extended and coherent, and the Hartree-Fock approximation of Leder[15] is valid. Only continuous valence transitions are possible in this case.

(2) If $U_{fd} \gg V$ the valence fluctuations are local and incoherent, and the f levels act like independent resonance levels. The problem of an isolated f level (impurity problem) is solved with more detail in the following paper. Within this picture discontinuous valence transitions occur if U_{fd} is sufficiently large.

For an actual physical situation we expect U_{fd}/V to be of the order of 10 to 10^2—hence the local approaches of Khomskii and Kocharjan[14] and Gonçalves da Silva and Falicov[17] are more appropriate descriptions of a mixed-valence compound than the calculation by Leder.[15]

The experimental situation seems to agree with this picture of independent and incoherent virtual-bound states: The specific heat shows a Schottky anomaly and a large low-temperature coefficient γ, $C = \gamma T$; the magnetic susceptibility is finite at zero temperatures and gradually goes over to a Curie-Weiss law when the temperature is raised; the dynamical susceptibility, as measured by inelastic neutron scattering, shows the $\vec{q}$ dependence of the ionic form factors[18]; and the valence transition may be continuous or discontinuous with pressure and temperature.

II. SPINLESS MODEL AND THE RENORMALIZATION GROUP

For spinless fermions the Hamiltonian, Eq. (1.1), reduces to

$$H = \sum_{\vec{k}} \epsilon_k d^\dagger_{\vec{k}} d_{\vec{k}} + E\sum_i f^\dagger_i f_i + V\sum_i (f^\dagger_i d_i + d^\dagger_i f_i) + U_{fd}\sum_i f^\dagger_i f_i d^\dagger_i d_i . \tag{2.1}$$

This model still contains the essential physics of the mixed-valence state. Beside the position of the f level with respect to the Fermi energy, the system is characterized by three energies, namely, the bandwidth D, the hybridization V, and the Coulomb repulsion U_{fd}.

The basic idea of scaling is to construct an effective Hamiltonian with a different band cutoff D' which describes the same physics as the original Hamiltonain. This can be achieved by correcting the coupling parameters V and U_{fd} and the energy E, which are now a function of D'. In other words, the scaling procedure is generated by integrating out degrees of freedom at the band edges and by obtaining in this way the renormalized effective-energy parameters of the system.

There are several methods to derive the scaling equations. In the present case the most convenient is the renormalization group. As for other infrared divergent models the problem can be formulated in terms of one dynamical variable. It is assumed that Green's functions, vertices, and other physical quantities obey a multiplicative renormalization[16]; i.e., for a quantity A we have

$$A[\omega/D'; U', V'] = zA[(\omega/D); U, V], \tag{2.2}$$

where z is a real factor and is independent of the

dynamical variable ω. As before, D' is the changed energy cutoff and U' and V' are the renormalized invariant couplings (we drop the suffix *fd* from now on). For any quantity obeying (2.2) a differential equation of the form

$$\frac{\partial}{\partial x}\ln A[x;U,V] = \frac{1}{x}\frac{\partial}{\partial \xi}\{\ln A[\xi;U'(x;U,V),V'(x;U,V)]\}_{\xi=1} \quad (2.3)$$

can be derived, where $x=\omega/D$. The initial condition for this Lie differential equation is

$$A[1;U,V]=1. \quad (2.4)$$

The prescription of the renormalization group[16] is now to calculate the perturbation expansion of the quantity A with respect to U and V and to insert this expression into the right-hand side of Eq. (2.3). The Lie differential equation then extends the skeleton diagrams included in the perturbation series consistently to all orders in U and V in the whole energy range.

We define the following dimensionless quantities $\tilde{\Gamma}$, $\tilde{\Lambda}$, d_d, and d_f:

$$\Gamma(\omega;U,V)=U\tilde{\Gamma}(\omega/D;U,V), \quad (2.5)$$

$$V^2\tilde{\Lambda}(\omega/D;U,V) = [\hat{V}(\omega/D;U,V)]^2 d_d(\omega/D;U,V)d_f(\omega/D;U,V), \quad (2.6)$$

$$G_d(\omega,\vec{k})=d_d(\omega/D;U,V)G_d^0(\omega,\vec{k}), \quad (2.7)$$

$$G_f(\omega,\vec{k})=d_f(\omega/D;U,V)G_f^0(\omega,\vec{k}), \quad (2.8)$$

where Γ is the four-leg vertex function which, in principle, is a function of three external energies and three momenta, G_d and G_f are the d and f particle propagators, and G_d^0 and G_f^0 are given by

$$G_d^0=(i\omega-\epsilon_k)^{-1}, \quad G_f^0=(i\omega-E)^{-1}. \quad (2.9)$$

$\hat{V}$ is the two-leg vertex function associated with the hybridization and $\tilde{\Lambda}$ is the derivative with respect to $\ln D/|\omega|$ of the response function $\langle\langle d_i^\dagger c_i^\dagger; f_i^\dagger d_i\rangle\rangle_\omega$. Equation (2.6) can be verified by comparing the perturbation expansion of $\tilde{\Lambda}$ with that of $\hat{V}^2 d_f d_d$. More rigorous arguments for the validity of this relation are given in the Appendix.

The above quantities $\tilde{\Gamma}$, d_d, d_f, $\hat{V}/V$, and $\tilde{\Lambda}$ obey multiplicative renormalization. This has been checked by perturbation theory up to third order in U and is shown more rigorously for some quantities in the Appendix. The renormalization of the hybridization vertex can be calculated either directly or through the correlation function $\langle\langle d_i^\dagger f_i; f_i^\dagger d_i\rangle\rangle_\omega$. We use the latter alternative.

The invariant couplings U' and V' are also assumed to satisfy condition (2.2) and hence the Lie differential Eq. (2.3). By requiring the invariance of the system under the renormalization transformation (2.2), i.e., $U'\tilde{\Gamma}G_dG_f$ and $(V'/V)^2\hat{V}^2G_dG_f$ are to be invariant, we obtain[16]

$$U'=U\frac{d_d(D'/D;U,V)}{d_d(1;U',V')}\frac{d_f(D'/D;U,V)}{d_f(1;U',V')}\frac{\tilde{\Gamma}(D'/D;U,V)}{\tilde{\Gamma}(1;U',V')} \quad (2.10)$$

and

$$(V')^2=V^2\frac{d_d(D'/D;U,V)}{d_d(1;U',V')}\frac{d_f(D'/D;U,V)}{d_f(1;U',V')}\left(\frac{\hat{V}(D'/D;U,V)}{\hat{V}(1;U',V')}\right)^2 = V^2\frac{\tilde{\Lambda}(D'/D;U,V)}{\tilde{\Lambda}(1;U',V')}. \quad (2.11)$$

These relations ensure the equivalence of the new system and the original one. The perturbation expansion for U' and V' can now be obtained from that of $\tilde{\Gamma}$, d_d, d_f, and $\tilde{\Lambda}$ or $\hat{V}$.

The validity of the assumption of multiplicative renormalization has been checked by perturbation theory for our model. In the Appendix we rederive diagramatically the scaling equations for the four-leg vertex in leading logarithmic order and for the hybridization vertex and the correlation $\tilde{\Lambda}$ in leading and next-leading logarithmic order. This can be considered as a formal proof of multiplicative renormalization within this logarithmic approximation. Comparing the results for $\tilde{\Lambda}$ and $\hat{V}$ we have also a verification for the validity of Eq. (2.6) up to the next-leading logarithmic order.

III. FIRST-ORDER RENORMALIZATION

Following the prescription of the renormalization-group technique we calculate the first-order corrections to $\tilde{\Gamma}$ and $\tilde{\Lambda}$. It is easily seen that d_d and d_f have only constant first-order corrections which can be absorbed into the chemical potential and a renormalization of E, respectively.

The first-order diagrams contributing to $\tilde{\Gamma}$ are shown in Fig. 1. We assume that we have one electron per site. Moreover, we add a small dispersion to the f-electron energy, which for the sake of simplicity we take as proportional to the d-electron dispersion ϵ_k:

$$E_k=E_0+\delta\epsilon_k, \quad |\epsilon_k|\le D, \quad |\delta|\ll 1. \quad (3.1)$$

If $\delta>0$ the f particles are electronlike, while if $\delta<0$ they have hole character. If $\delta=0$ they are completely localized.

FIG. 1. Second-order vertex diagrams. The dashed lines represent f-electron propagators and the full lines represent d-electron propagators.

Let us first discuss the dependence of the vertex $\tilde{\Gamma}$ on the sign of δ for $E_0 = 0$ and return to the general case later. The evaluation of the diagrams is straightforward and we have

$$\tilde{\Gamma} = 1 - 2\frac{U\rho_F}{1+|\delta|}\,\mathrm{sgn}\delta\,\ln[(1+|\delta|)D/|\omega|]\,, \tag{3.2}$$

where sgnδ takes the values $+1$, -1, and 0, depending on whether it is positive, negative, or zero, respectively. The perturbation expansion for the invariant coupling U' is obtained via Eq. (2.10):

$$U' = U + 2\frac{U^2\rho_F}{1+|\delta|}\mathrm{sgn}\delta\,\ln(D'/D)\,. \tag{3.3}$$

Inserting this expression into Eq. (2.3) we have

$$\frac{dU'}{d\,\ln(D'/D)} = \frac{2\rho_F}{1+|\delta|}\mathrm{sgn}\delta\,U'^2\,, \tag{3.4}$$

which when integrated with the condition $U'(D'=D) = U$ yields

$$U' = U\Big/\left(1+\frac{2U\rho_F}{1+|\delta|}\,\mathrm{sgn}\delta\,\ln(D/D')\right). \tag{3.5}$$

This expression decreases when D' is reduced if $U\delta$ is positive, i.e., the f and d bands are weakly coupled through U. If $U\delta$ is negative the invariant coupling grows, and we have strongly coupled f and d bands; in the case $\delta = 0$, U' remains equal to its bare value U.

Similarly, we calculate the invariant coupling associated with V. The perturbation expansion for the correlation $\langle\langle d_i^\dagger f_i; f_i^\dagger d_i\rangle\rangle_\omega$ up to first order is seen in Fig. 2. The correction vanishes if $\delta > 0$; we have in general

$$\tilde{\Lambda} = 1 + \frac{2U\rho_F}{1+|\delta|}(1-\mathrm{sgn}\delta)\,\ln[(1+|\delta|)D/|\omega|]\,. \tag{3.6}$$

The perturbation expansion for $(V')^2$ is obtained via Eq. (2.11):

$$(V')^2 = V^2\left(1 - \frac{2U\rho_F}{1+|\delta|}(1-\mathrm{sgn}\delta)\ln(D'/D)\right), \tag{3.7}$$

which when inserted into the right-hand side of Eq. (2.3) yields

$$\frac{dV'}{d\,\ln(D'/D)} = -(1-\mathrm{sgn}\delta)\frac{V'U'\rho_F}{1+|\delta|}\,. \tag{3.8}$$

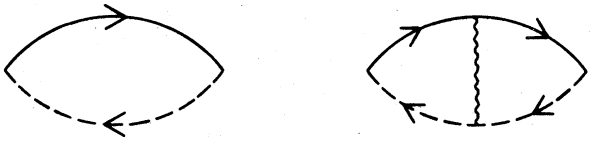

FIG. 2. Bare and first-order diagrams of the correlation $\langle\langle d_i^\dagger f_i; f_i^\dagger d_i\rangle\rangle_\omega$.

Integrating this equation using Eq. (3.5) we have

$$\frac{V'}{V} = \left(1 - \frac{2U\rho_F}{1+|\delta|}\ln(D/D')\right)^{-1} = \frac{U'}{U} \quad \text{if } \delta < 0\,, \tag{3.9}$$

$$\frac{V'}{V} = \left(\frac{D}{D'}\right)^{U\rho_F} \quad \text{if } \delta = 0\,, \tag{3.10}$$

and

$$\frac{V'}{V} = 1 \quad \text{if } \delta > 0\,. \tag{3.11}$$

Hence, if $\delta > 0$, V' remains equal to its bare value V, while if $\delta \leq 0$ the hybridization is enhanced if $U > 0$. The enhancement for $\delta = 0$, however, is qualitatively different from that for $\delta < 0$.

In conclusion, for repulsive U (> 0) and an electronlike f band the system is weakly coupled. On the other hand, a holelike or a dispersionless f band is strongly coupled to the d-electron band. Hence, the results depend qualitatively on the sign of δ, the point $\delta = 0$ being singular.

The Hamiltonian can be diagonalized for $U = 0$; for $\delta = 0$ the hybridization opens a gap at the Fermi level. The diagrams of Figs. 1 and 2 evaluated with a small hybridization yield the same results as for a holelike f band. Hence, in the case of a dispersionless f band we have to take the limit $\delta \to 0-$ (f-hole band) in order to reproduce the results for $U = 0$, $V \to 0$. In general, we can say that we have strong coupling if there is a hybridization gap and weak coupling if there is no gap in the spectrum.

The scaling condition requires that only one energy scale play a role in the problem. This is the reason why we do not consider the part of (2.1) bilinear in fermion operators as the unperturbed Hamiltonian and U as the only perturbation. In this case the hybridization gap would be the second energy scale.

In summary, if we consider a coherent hybridization model, the diagrams are to be evaluated in the limit $\delta \to 0-$; on the other hand, for local and incoherent valence fluctuations the case $\delta = 0$ must be taken.

IV. RENORMALIZATION FOR EXTENDED AND COHERENT STATES

With the above criterion for coherent hybridization states and for an arbitrary E_0 we obtain

$$U' = U/[1 - 2U\rho_F \ln(D/D')]\,, \quad V'U = VU' \tag{4.1}$$

$$\tilde{\Gamma}\left(\frac{\omega}{D}\right) = [1 - 2U\rho_F\ln(D/|\omega|)]^{-1}\,, \quad \tilde{\Lambda}\left(\frac{\omega}{D}\right) = \tilde{\Gamma}^2\left(\frac{\omega}{D}\right). \tag{4.2}$$

The result is equivalent to summing up the most singular contributions in the logarithmic approximation (see Appendix). The validity of the scaling

equations (4.1) is restricted to small values of U'; otherwise, higher-order skeleton diagrams have to be taken into account in Eqs. (3.4) and (3.8). With (4.1) we can state, however, that the system has no fixed point for small U (>0). This result cannot be changed by higher-order contributions.

Let us relate the leading-logarithmic-order results to the Hartree-Fock approximation[15] for extended states. From Eq. (3.4) we see that for $\delta<0$ the fixed point is given by $U'=\infty$, i.e., we obtain a characteristic energy of the Bardeen-Cooper-Schrieffer (BCS) type:

$$T_0 = De^{-1/(2U\rho_F)}. \tag{4.3}$$

The Hartree-Fock equation for the effective hybridization is obtained from Eq. (3.9), which can be rewritten as

$$V^* = V + 2U\rho_F V^* \ln(D/V^*), \tag{4.4}$$

where we replaced D' by V^*. The validity of the Hartree-Fock approximation is, of course, restricted to small U.

We proceed to evaluate the next-leading contributions in the logarithmic approximation. The self-energy graphs shown in Fig. 3 have to be considered for the cases

$$\Sigma_f = -2(i\omega - E_0)U^2\rho_F^2 \ln(D/|\omega|) \tag{4.5}$$

and

$$\Sigma_d = -2(i\omega - \epsilon_k)U^2\rho_F^2 \ln(D/|\omega|), \tag{4.6}$$

where the diagrams were evaluated in the limit $\delta \to 0-$. From (4.5) and (4.6) we obtain the perturbation expansions for the factors d_f and d_d:

$$d_f = d_d = 1 - 2U^2\rho_F^2 \ln(D/|\omega|). \tag{4.7}$$

It is seen that d_f and d_d decrease if $|\omega|$ is lowered.

In order to evaluate the next-leading corrections to $\tilde{\Gamma}$ we note that only diagrams with a closed fermion loop yield a new contribution, which is not contained in the renormalization of the diagrams of Fig. 1. The diagrams are shown in Fig. 4, and we have

$$\tilde{\Gamma} = 1 + 2U\rho_F \ln(D/|\omega|) + 4U^2\rho_F^2 \ln(D/|\omega|). \tag{4.8}$$

As a consequence the invariant coupling U' is not renormalized in next-leading order:

$$U' = U - 2U^2\rho_F \ln(D'/D), \tag{4.9}$$

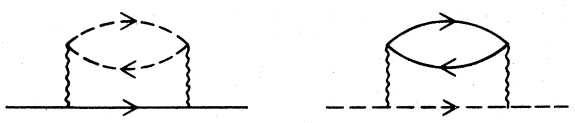

FIG. 3. Second-order self-energy diagrams.

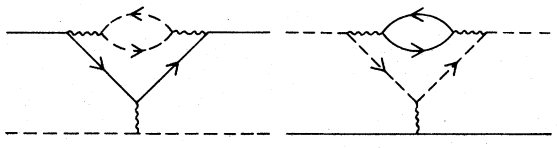

FIG. 4. Third-order vertex diagrams that contribute in next-leading logarithmic approximation.

due to the Ward cancellation of the vertex and self-energy diagrams.

In a similar way we obtain the corrections to $\tilde{\Lambda}$ by evaluating the diagrams of Fig. 5:

$$\tilde{\Lambda} = 1 + 4U\rho_F \ln(D/|\omega|) - 4U^2\rho_F^2 \ln(D/|\omega|). \tag{4.10}$$

Using Eq. (2.11) we see that the hybridization is reduced with respect to Eq. (4.1) by the next-leading logarithmic approximation

$$\frac{U'}{U} = \frac{1}{1 - 2U\rho_F \ln(D/D')}, \quad \frac{V'}{V} = \frac{U'}{U}\left(\frac{D'}{D}\right)^{2U'U\rho_F^2}. \tag{4.11}$$

So far we considered only local correlations. Since the f electrons are very heavy the interactions between different sites are mediated only by the d electrons. There is no interaction among sites in leading logarithmic order. The most important interaction (next-leading order) is of the Ruderman-Kittel-Kasuya-Yosida (RKKY) type and is shown in Fig. 6:

$$3\pi(1-n_f)\rho_F[U\tilde{\Gamma}(\omega/D)]^2 F(2k_F R_{ij}) f_i^\dagger f_i f_j^\dagger f_j, \tag{4.12}$$

where $F(2k_F R)$ is the space dependence of the RKKY interaction.

We conclude that the leading-order results are not essentially changed by the next-leading logarithmic renormalization. They are valid for small U. With growing U, correlations among the sites become important. If these correlations are comparable or larger than the bare hybridization V, the f states should no longer be considered as a band. In this case fluctuations are larger than the "f-band" dispersion and the $\vec{k}$ space is not a convenient basis to start a perturbation. Rather than calculating the perturbation within an extended-state picture, the f level should be treated as a localized

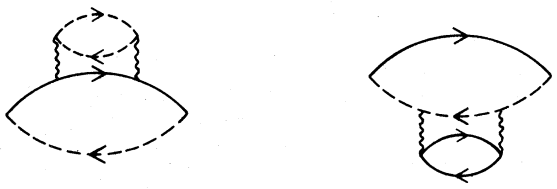

FIG. 5. Second-order diagrams contributing to $\langle\langle d_i^\dagger f_i; f_i^\dagger d_i\rangle\rangle_\omega$.

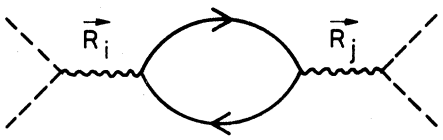

FIG. 6. Diagram generating the RKKY interaction.

state. In other words, instead of using the prescription of taking the limit $\delta \to 0-$ as described in Sec. III, we should consider the case $\delta = 0$. We discuss the renormalization within the local picture in Sec. V.

We would like to mention that by solving the model at the leading-order fixed point we obtain that the local correlations are dominant and that the state of lowest energy has one electron per site,

$$(\epsilon^2 + V^{*2})^{-N/2} \prod_i (V^* d_i + \epsilon f_i)|0\rangle , \tag{4.13}$$

where $|0\rangle$ is the vacuum state and N is the number of sites. Its energy is given by $N\epsilon$, where

$$\epsilon = \tfrac{1}{2}[E - (E^2 + 4V^{*2})^{1/2}] . \tag{4.14}$$

Here V^* is defined by Eq. (4.4). This is essentially the model solved by Gonçalves da Silva and Falicov.[17] These single-site states are in addition strongly correlated via the RKKY interaction (4.12).

V. RENORMALIZATION WITHIN THE LOCAL PICTURE

If we consider a model with strictly localized f electrons, the results of the renormalization are very different, as seen in Sec. III. We see from Eqs. (3.2)–(3.5) that the two bubbles of Fig. 1 cancel each other for $\delta = 0$. As a consequence the invariant coupling U' remains equal to its bare value in leading logarithmic order.

In the same way, we have from the diagrams of Fig. 2 that for $\delta = 0$ the function $\tilde{\Lambda}$ takes the form

$$\tilde{\Lambda}(\omega/D) = (D/|\omega|)^{2U\rho_F} , \tag{5.1}$$

and that V' is renormalized by a power of D/D' [see Eq. (3.10)]. In this case we obtain no BCS-type pole, but in analogy to Eq. (4.4) we are able to define an effective hybridization

$$V^* = V(D/V^*)^{U\rho_F} \quad \text{or} \quad V^* = V(D/V)^{U\rho_F/(1+U\rho_F)} . \tag{5.2}$$

We now proceed to evaluate the next-leading logarithmic corrections to the self-energies and the vertex. For the f-electron self-energy we obtain

$$\Sigma_f = -(i\omega - E_0)U^2\rho_F^2 \ln(D/|\omega|) , \tag{5.3}$$

and the d-electron self-energy can be approximated by

$$\Sigma_d = -i\pi U^2 \rho_F n_f (1 - n_f) . \tag{5.4}$$

Hence Σ_d does not contribute to next-leading logarithmic renormalization and we have

$$d_d = 1, \quad d_f = 1 - U^2\rho_F^2 \ln(D/|\omega|) . \tag{5.5}$$

Only one diagram of Fig. 4 contributes to $\tilde{\Gamma}$ in next-leading order

$$\tilde{\Gamma} = 1 + U^2\rho_F^2 \ln(D/|\omega|) , \tag{5.6}$$

and due to the Ward cancellation of vertex and self-energies we have

$$U' = U , \tag{5.7}$$

also in next-leading order. In the same way we obtain

$$\tilde{\Lambda} = 1 + 2U\rho_F \ln(D/|\omega|) - U^2\rho_F^2 \ln(D/|\omega|) , \tag{5.8}$$

such that Eqs. (3.10) and (5.2) are only slightly modified: $U\rho_F$ has to be replaced by $U\rho_F(1 - \frac{1}{2}U\rho_F)$. Also Eq. (4.12) remains valid if $\tilde{\Gamma}$ is replaced by 1.

The above results are qualitatively different from those of Sec. IV. In the extended and coherent mixed-valence picture the vertex has a pole which determines an effective hybridization. This approach is certainly correct if the hybridization gap is larger than the fluctuations in the system, i.e., if $V \gg U$. In this case U is a small parameter and the perturbation expansion converges. On the other hand, in the local and incoherent mixed-valence picture the f levels behave essentially like independent impurities. The local picture is certainly more adequate if $V \ll U$, since in this case the correlations among sites are larger than the "f-band dispersion" and, as a consequence of the strong dependence of Eqs. (3.2)–(3.11) on the sign of δ, U can no longer be considered as a small parameter. In the actual physical situation we expect to have $U \gg V$. We discuss the corresponding impurity model in detail in the following paper.

VI. CONCLUSIONS

In this paper we considered a model with spinless extended and localized electrons. Neglecting the spins represents a large simplification of the Anderson lattice, since the model now only involves charge fluctuations, but it still contains the main feature of valence instabilities, namely, the competition between two atomic configurations with similar energies.

The main problem we faced in this paper is the question whether the mixed-valence state is an extended coherent-hybridization state or if the

"valence fluctuations" of the rare-earth (RE) ions are rather local and incoherent. In both cases, the coherent and the local picture, the perturbation expansion with respect to U shows logarithmic infrared divergences; the results, however, are very different. The coherence of the states are triggered by the hybridization V, whereas the interaction U induces fluctuations which tend to destroy the coherence.

In Sec. IV we discussed the case of extended states. The coherence of the states is simulated by a model with an f band of very heavy holes ($\delta < 0$) and V considered as an external perturbation. The invariant coupling U' has a pole at $T_0 = D\exp[-1/(2U\rho_F)]$, in analogy to the BCS theory, and at the fixed point we recover the self-consistent Hartree-Fock equation for the effective hybridization, Eq. (4.4). The next-leading logarithmic approximation yields intersite interactions of the RKKY type among the f holes. The strength of these intersite correlations is proportional to U'^2.

In the framework of local and incoherent valence fluctuations the f band has no dispersion ($\delta = 0$). The renormalization procedure yields an enhanced hybridization V', while the invariant coupling U' remains equal to its bare value U. The results of the renormalization are similar to those of an isolated f level. In nonleading logarithmic approximation intersite RKKY interactions are built up with a strength proportional to U^2. The lifetime of the conduction electrons is considerably reduced, Eq. (5.6); it screens the RKKY interaction at large distance such that the correlation between f electrons at different sites is short ranged.

In order to interpret our results physically we distinguish the cases $U \ll V$ and $U \gg V$. The invariant coupling V' is a measure for the coherence of the state, whereas U' characterizes the multiple single-site scattering, i.e., the local correlations, and U'^2 RKKY the many-site scattering, i.e., the nonlocal correlations.

If $U \ll V$, we have for $V' < D'$ from Eqs. (4.1), (4.4), and (4.11) that $U' \ll V'$, i.e., that the effective hybridization is more important than the fluctuations in the extended-state picture. In other words, the renormalization of coherent states yields again coherent states. On the other hand, the renormalization in the local picture yields small fluctuations and a large hybridization, such that coherent states must develop. Hence, one drives from the local picture to the extended picture. An alternative way to arrive at this conclusion is to compare the ground-state energies when the fluctuations are neglected. A coherent hybridization reduces the energy-per-site proportionality to V', while the local resonance levels yield an energy gain of only $V'^2\rho_F$.

If $U \gg V$, the local and nonlocal correlations are dominant in the extended-state picture, Eqs. (4.11) and (4.12). These large fluctuations destroy the coherence of the states, and the renormalization drives the system to the local incoherent picture. In this case the fluctuations require a large energy compared to the energy gain provided by the coherent hybridization. On the other hand, in the local- and incoherent-states framework, the nonlocal correlations are small, such that each RE ion behaves essentially as an isolated impurity. Since $U \gg V$ the multiple single-site scattering still dominates over the hybridization such that the system remains within this picture when renormalized.

In physical systems we expect the Falicov-Kimball interaction U to be of the order of 1 eV and a hybridization of a few percent of eV. With these values for the energy parameters we expect local and incoherent valence fluctuations; in other words, a mixed valence compound behaves like a system of essentially isolated impurities. This picture agrees with that arising from the experiment, i.e., thermodynamical properties and the $\vec{q}$ dependence of the inelastic neutron scattering cross section, which is given by the ionic form factor.[18] The solution of the f-level impurity problem is discussed in the following paper.

In summary, we have to distinguish three regimes: (a) if $U \ll V$, the mixed-valence state is extended and coherent; (b) if $U \gg V$, the valence fluctuations are local and incoherent; and (c) the crossover region for intermediate ratios of U/V. This crossover regime is physically different from the other two and could give a possible explanation for some properties of systems like SmB_6.

Notes added in proof. If the spin degree of freedom is included the large Coulomb repulsion U_{ff} between f electrons with opposite spin provides an additional mechanism to break the coherence of the extended states. This can be seen from the fact that the leading logarithmic divergences are due to single-site correlations.[4]

There is an approximation involved in the calculation within the extended picture. The momentum integrations over the Fermi sphere depend on the choice of the band structure. Hence, the problem is not universal. Moreover, it is essential for the validity of multiplicative renormalization to consider the quantities d_f, d_d, $\hat{V}$, and $\tilde{\Gamma}$ as independent on the momentum variables. This has been assumed throughout the paper. With this approximation tedious integrations over the Fermi sphere are avoided. We do not expect the results to change qualitatively with a more careful treatment of the momentum dependence. The renorm-

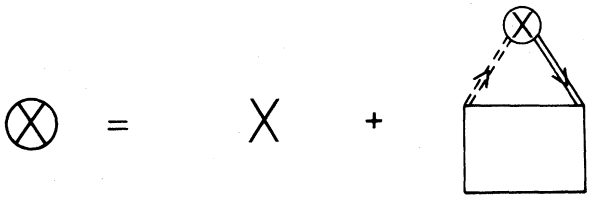

FIG. 7. Integral equation for the renormalized hybridization vertex.

alization within the local picture is not affected by this approximation.

APPENDIX

We present here a diagramatic derivation of the scaling laws for some of the quantities defined in Sec. II. This derivation is independent of the assumption of multiplicative renormalization and can be considered as a proof for its validity. The diagramatic calculation is tedious, and much care must be taken with the logarithmic variables. The renormalization group is an alternative method which straightly and safely yields the same results.

We first derive the scaling equation of the four-leg vertex in leading logarithmic order. The vertex is in principle a function of three energy variables. In general we have to consider two scattering channels termed in the literature as the zero-sound and Cooper channels.[16,19,20] Following, for instance, Refs. 19 and 20, one has to define irreducible vertex blocks within these channels and set up the parquet equations. The parquet equations are a coupled set of integral equations whose solutions yield the vertex as a function of the three energy variables. This procedure is tedious, and it can be simplified using the Sudakov-Abrikosov[19,21,22] trick. By means of this trick the parquet equations for the vertex depending on three energy variables is reduced to an integral equation for a vertex function depending on a single energy variable,

$$\tilde{\Gamma}=1-\frac{U\rho_F}{1+|\delta|}(1+\mathrm{sgn}\delta)\int_{|\omega|}^{D}d\omega_1\frac{1}{\omega_1}\tilde{\Gamma}^2(\omega_1)+\frac{U\rho_F}{1+|\delta|}(1-\mathrm{sgn}\delta)\int_{|\omega|}^{D}d\omega_1\frac{1}{\omega_1}\tilde{\Gamma}^2(\omega_1)\,. \tag{A1}$$

This equation corresponds to the diagrams of Fig. 1 with the interaction lines replaced by a full vertex function. We restricted ourselves to the case $E_0=0$ in leading logarithmic order discussed in Sec. III. Taking the derivative with respect to ω we obtain

$$\frac{d\tilde{\Gamma}}{d\ln(|\omega|/D)}=\frac{2U\rho_F}{1+|\delta|}(\mathrm{sgn}\delta)\,\tilde{\Gamma}^2\,. \tag{A2}$$

Since in leading order $U'=U$, this equation is equivalent to (3.4) and (3.5).

We proceed now to calculate the hybridization vertex in leading and next-leading logarithmic order. The integral equation determining $\hat{V}$ is diagramatically shown in Fig. 7. Here $\hat{V}$ is denoted by an encircled cross, the bare V by a cross, the four-leg vertex by a square, and the dressed propagators by the double lines. It is sufficient to consider $\tilde{\Gamma}$ as a function of a single energy variable. Within the logarithmic approximation the integral equation can be reduced to

$$\hat{V}(\omega)=V+\frac{U\rho_F}{1+|\delta|}(1-\mathrm{sgn}\delta)\int_{|\omega|}^{D}d\omega_1\frac{1}{\omega_1}d_d(\omega_1)d_f(\omega_1)\tilde{\Gamma}(\omega_1)\hat{V}(\omega_1)\,. \tag{A3}$$

Taking the derivative with respect to ω we obtain

$$\frac{d\ln\hat{V}(\omega)}{d\ln(|\omega|/D)}=-\frac{1-\sin(\delta)}{1+|\delta|}U\rho_F\tilde{\Gamma}(\omega)d_d(\omega)d_f(\omega)=-\frac{1-\mathrm{sgn}\delta}{1+|\delta|}U'\rho_F\,. \tag{A4}$$

This equation is equivalent to (3.8), (4.11), and (5.2).

Let us finally consider the function $\tilde{\Lambda}$. The response function $\langle\langle d_i^\dagger f_i; f_i^\dagger d_i\rangle\rangle_\omega$ is obtained by evaluating the diagrams of Fig. 2 with dressed propagators and the interaction line replaced by a full vertex function depending on three energy variables. In leading logarithmic order we have

$$\langle\langle d_i^\dagger f_i; f_i^\dagger d_i\rangle\rangle_\omega=-\rho_F\frac{1-\mathrm{sgn}\delta}{1+|\delta|}\eta+\rho_F^2U\left(\frac{1-\mathrm{sgn}\delta}{1+|\delta|}\right)^2\int_0^\eta dt_1\int_0^\eta dt_2\hat{\Gamma}(t_1,t_2,\eta)\,, \tag{A5}$$

where $\eta=\ln D/|\omega|$ and t are logarithmic energy variables and $\hat{\Gamma}$ is the vertex Γ depending on three energy variables. It is now necessary to make a similar reduction as the Sudakov-Abrikosov trick for the vertex. The procedure is tedious and can be taken from Appendix A of Ref. 20. We obtain finally

$$\tilde{\Lambda}(\omega)=\exp\left(2U\rho_F\frac{1-\mathrm{sgn}\delta}{1+|\delta|}\int_{|\omega|}^{D}dx\frac{1}{x}\tilde{\Gamma}(x)\right). \tag{A6}$$

The derivative with respect to ω yields the scaling equation

$$\frac{\partial \ln\tilde{\Lambda}}{\partial \ln(|\omega|/D)} = -2U\rho_F \frac{1-\mathrm{sgn}\delta}{1+|\delta|}\,\tilde{\Gamma}(\omega) = -2U'\rho_F \frac{1-\mathrm{sgn}\delta}{1+|\delta|}. \tag{A7}$$

This equation is equivalent to (4.2) and (5.1).

The self-energies contribute to the next-leading logarithmic order and Eq. (A5) is modified to

$$\langle\langle d_i^\dagger f_i; f_i^\dagger d_i\rangle\rangle_\omega = -\rho_F \frac{1-\mathrm{sgn}\delta}{1+|\delta|}\int_0^\eta dt\, d_d(t)d_f(t) + \rho_F^2 U\left(\frac{1-\mathrm{sgn}\delta}{1+|\delta|}\right)^2 \int_0^\eta dt_1 d_d(t_1)d_f(t_1)\int_0^\eta dt_2 d_d(t_2)d_f(t_2)\hat{\Gamma}(t_1,t_2,\eta). \tag{A8}$$

By the above procedure this equation is reduced to

$$\frac{\tilde{\Lambda}(\omega)}{d_d(\omega)d_f(\omega)} = \exp\left(2U\rho_F \frac{1-\mathrm{sgn}\delta}{1+|\delta|}\int_{|\omega|}^D dx \frac{1}{x}\,\tilde{\Gamma}(x)d_d(x)d_f(x)\right), \tag{A9}$$

and we finally obtain

$$\frac{\partial \ln(\tilde{\Lambda}/d_f d_d)}{\partial \ln(|\omega|/D)} = -2U\rho_F \frac{1-\mathrm{sgn}\delta}{1+|\delta|}\,\tilde{\Gamma}(\omega)d_d(\omega)d_f(\omega) = -2U'\rho_F \frac{1-\mathrm{sgn}\delta}{1+|\delta|}. \tag{A10}$$

Comparing Eqs. (A4) and (A10) we obtain that

$$\hat{V}^2(\omega) = (\mathrm{const})\tilde{\Lambda}(\omega)/d_f(\omega)d_d(\omega). \tag{A11}$$

The proportionality constant is fixed by setting $\omega = D$ to be V^2. Herewith we have proved Eq. (2.6) up to next-leading logarithmic order.

---

[1] J. M. Robinson, Physics Reports 51, 1 (1979).
[2] R. Ramirez, L. M. Falicov, and J. C. Kimball, Phys. Rev. B 2, 3383 (1970).
[3] B. Alascio, A. López, and C. F. E. Olmedo, J. Phys. F 3, 1324 (1973).
[4] A. Bringer and H. Lustfeld, Z. Physik B 28, 213 (1977).
[5] H. J. Leder and B. Mühlschlegel, Z. Phys. B 29, 341 (1978).
[6] C. E. T. Gonçalves da Silva and L. M. Falicov, J. Phys. C 5, 906 (1972).
[7] R. M. Martin and J. W. Allen, Bull. Am. Phys. Soc. 24, 395 (1979).
[8] H. J. Leder and G. Czycholl, Z. Phys. B 35, 7 (1979).
[9] M. E. Foglio and L. M. Falicov, Phys. Rev. B 20, 4554 (1979); M. E. Foglio, C. A. Balseiro, and L. M. Falicov, Phys. Rev. B 20, 4560 (1979).
[10] P. Schlottmann, Phys. Rev. B 19, 5036 (1979).
[11] B. Batlogg, E. Kaldis, A. Schlegel, G. von Schulthess, and P. Wachter, Solid State Commun. 19, 673 (1976).
[12] R. Jullien, J. N. Fields, and S. Doniach, Phys. Rev. B 16, 4889 (1977).
[13] C. Lacroix and M. Cyrot, Phys. Rev. B 20, 1965 (1979).
[14] D. I. Komskii and A. N. Kocharjan, Solid State Commun, 18, 935 (1976).
[15] H. J. Leder, Solid State Commun. 27, 579 (1978).
[16] N. Menyhárd and J. Sólyom, J. Low Temp. Phys. 12, 529 (1973).
[17] C. E. T. Gonçalves da Silva and L. M. Falicov, Solid State Commun. 17, 1521 (1975).
[18] E. Holland-Moritz, M. Loewenhaupt, W. Schmatz, and D. Wohlleben, Phys. Rev. Lett. 38, 983 (1977); S. M. Shapiro, J. D. Axe, R. J. Birgenau, J. M. Lawrence, and R. D. Parks, Phys. Rev. B 16, 2225 (1977).
[19] B. Roulet, J. Gavoret, and P. Nozières, Phys. Rev. 178, 1072 (1969).
[20] R. Gerhardts and P. Schlottmann, Z. Phys. B 34, 349 (1979).
[21] V. V. Sudakov, Dok. Akad. Nauk SSSR 111, 338 (1956) [Sov. Phys. Dokl. 1, 662 (1956)].
[22] A. A. Abrikosov, Physics (N.Y.) 2, 5 (1965).